Effects of threshold retrievals on estimates of the aerosol indirect radiative forcing

Mark A. Matheson,[1,2] James A. Coakley Jr.,[1] and William R. Tahnk[1]

Received 25 December 2005; revised 30 January 2006; accepted 24 February 2006; published 4 April 2006.

[1] Empirical estimates of the aerosol indirect radiative forcing often rely on threshold cloud retrievals applied to multispectral satellite imagery data. In such retrievals, pixels having radiances that surpass prescribed thresholds are assumed to be overcast even if they are only partially cloud covered. This assumption leads to cloud visible optical depths that are underestimated and droplet radii that are overestimated. As regional cloud cover increases, overcast pixels become more common and the biases in cloud properties decrease. Because aerosol optical depths derived from cloud-free pixels also increase with regional cloud cover (Loeb and Manalo-Smith, 2005), the biases in threshold-derived cloud properties can be mistakenly interpreted as being evidence for the effects of aerosols on clouds. Because of the biases, threshold retrievals of cloud properties are likely to lead to overestimates of the aerosol indirect forcing. A retrieval scheme that accounts for fractional cloud cover within an imager pixel is used to estimate the enhancement in the indirect radiative forcing that arises from threshold cloud retrievals. The enhancements prove to be relatively small, approximately 20%. If cloud liquid water is held fixed to estimate the forcing, the biases in threshold-derived droplet radii and in the sensitivity of droplet radii to changes in aerosol nearly cancel so that the estimates are almost the same for threshold and partly cloudy pixel retrievals. **Citation:** Matheson, M. A., J. A. Coakley Jr., and W. R. Tahnk (2006), Effects of threshold retrievals on estimates of the aerosol indirect radiative forcing, *Geophys. Res. Lett.*, *33*, L07705, doi:10.1029/2005GL025614.

1. Introduction

[2] A number of studies have sought to use multispectral satellite imagery data to estimate the aerosol indirect radiative forcing [*Kaufman and Nakajima*, 1993; *Kaufman and Fraser*, 1997; *Wetzel and Stowe*, 1999; *Nakajima et al.*, 2001; *Sekiguchi et al.*, 2003; *Quaas et al.*, 2004]. While some of these studies applied measures of spatial uniformity in infrared emission to ensure that the pixels being analyzed were overcast [*Wetzel and Stowe*, 1999; *Nakajima et al.*, 2001], for the most part the studies used threshold cloud retrievals to derive the cloud properties.

[3] Recently, *Coakley et al.* [2005] developed a retrieval scheme that explicitly accounts for partly cloudy imager pixels. They showed that threshold retrievals generally overestimate droplet effective radius and underestimate cloud optical depth, liquid water path, and column number concentration. *Matheson et al.* [2005] and M. A. Matheson et al. (Multiyear AVHRR observations of summertime stratocumulus collocated with aerosols in the northeastern Atlantic, submitted to *Journal of Geophysical Research,* 2005, hereinafter referred to as Matheson et al., submitted manuscript, 2005) used the partly cloudy pixel retrieval algorithm to investigate the aerosol indirect radiative forcing by examining changes in cloud properties in response to changes in aerosol optical depth. Here, aspects of the study are repeated using threshold retrievals for the cloud properties to determine how the threshold-derived properties affect estimates of the aerosol indirect radiative forcing. While previous studies relied on correlations of cloud properties with a measure of aerosol column amount to infer the effects of aerosols on clouds, *Matheson et al.* [2005] identified a number of physical processes that could give rise to correlations that mimic effects expected for enhanced particle concentrations in clouds, but which, in fact, may have little to do with the aerosol indirect radiative forcing. Nonetheless, correlations like those used in previous studies will be used here to compare estimates of the aerosol indirect radiative forcing derived using threshold retrievals with those derived using partly cloudy pixel retrievals.

2. Data and Methodology

[4] The methodology used in the current study is briefly described. A complete description is given by *Matheson et al.* [2005, also submitted manuscript, 2005]. All daytime 4-km Global Area Coverage (GAC) data for May-August 1995–1999 from the AVHRR on the NOAA 14 satellite were analyzed for the northeastern Atlantic bounded by 35°–55° N latitude and 0°–20° W longitude. Only ocean pixels were used and those that were within 40° of the sun's reflection, assuming specular reflection from a flat surface and thus probably affected by sun glint, were removed from further analysis.

[5] A scene identification scheme was used to identify 4-km pixels as cloud-free, partially covered by clouds, completely overcast by clouds in a single layer, or containing clouds that were distributed in altitude. Details of the scene identification and the retrieval of cloud properties for single-layered cloud systems for both overcast and partly cloudy pixels are given by *Coakley et al.* [2005]. For cloud-free pixels, a scheme developed for the Indian Ocean Experiment (INDOEX) was used to derive aerosol optical depths [*Coakley et al.*, 2002].

[1]College of Oceanic and Atmospheric Sciences, Oregon State University, Corvallis, Oregon, USA.

[2]Now at Building Research Institute, Department of Environmental Engineering, Tsukuba, Japan.

0094-8276/06/2005GL025614$05.00

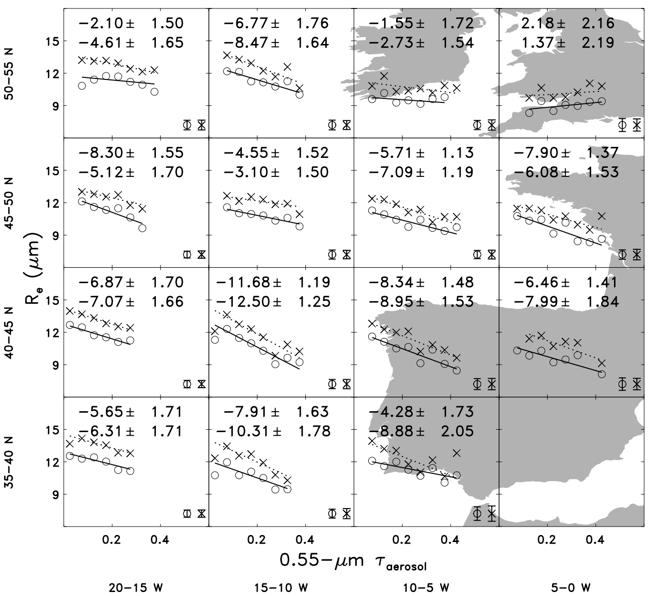

Figure 1. Means of overpass averaged droplet effective radius (μm) for 1° regions binned for each 0.05 interval of 0.55-μm aerosol optical depth. Each sub-panel contains observations for that 5° region. Circles represent partly cloudy pixel retrievals, crosses represent threshold retrievals. Error bars in the lower right corner are the RMS of the standard errors of the means for the data points. These errors result from statistical sampling and do not represent errors in the retrievals. The solid (dashed) line is a linear fit to the bin means of the circles (crosses) inversely weighted by the standard errors. Also given are the mean and standard deviation estimated for the slope of the linear fit to the circles (upper) and crosses (lower).

[6] In order to simulate threshold retrievals, radiances for pixels having fractional cloud cover greater than 0.20 were used as inputs to the overcast retrieval scheme to calculate a new set of cloud properties. As was noted by *Coakley et al.* [2005], taking as overcast pixels with fractional cloud cover greater than 0.2 produces a cloud mask like that obtained using the International Satellite Cloud Climatology Project thresholds described by *Rossow and Garder* [1993]. In addition, when pixel-scale cloud cover is small, large errors arise in the retrieved cloud properties owing to uncertainties in the radiances associated with the cloud-free portion of the pixel and in the cloud layer altitude. Consequently, pixels with fractional cloud cover less than 0.20 were removed from the data for both the partly cloudy pixel and threshold retrieval schemes.

[7] Pixel-scale observations for each satellite pass were mapped into 1° × 1° latitude-longitude regions. The cloud screening rules described by *Matheson et al.* [2005] were used to select 1° regions in which 1) all clouds were part of a single-layered, low-level cloud system and 2) the region had sufficient numbers of cloudy and cloud-free pixels to allow reliable determination of the average cloud and aerosol properties within the region. For each overpass and 1° region, the average cloud properties were obtained by weighting the pixel-scale values by the pixel-scale fractional cloud cover.

[8] For each overpass, the means of the 1° regions were gathered into 5° × 5° latitude-longitude regions in order to increase the number of samples exhibiting relatively homogeneous aerosol and cloud properties and to avoid, to the extent possible, the effects of geographic gradients in the cloud and aerosol properties observed for the northeastern Atlantic. Matheson et al. (submitted manuscript, 2005) demonstrated that the means and standard deviations of the cloud and aerosol properties within the 5° regions were consistent from year to year and that the inter-annual variability was much smaller than the day-to-day variability. The year-to-year consistency of the cloud and aerosol properties justified combining all five years of data into a single ensemble for each 5° region.

3. Collocated Aerosol Optical Depths and Cloud Properties

[9] Figures 1–3 show the mean properties and the standard error of the means for low-level, single-layered clouds in each 5° region and each 0.05 wide bin of the associated 0.55-μm aerosol optical depth. The standard error of the mean is the statistical sampling error, and is given by the standard deviation divided by the square-root of the number of independent samples, in this case, the number of satellite overpasses that contributed observations to that aerosol optical depth bin. Bins with overpass means from fewer than 10 separate satellite overpasses were excluded. The slope and standard error of the slope for the trends were estimated from a linear fit to the bin means weighted by the inverse of the standard errors of the bin means [*Bevington*, 1969]. One 5° region had means from fewer than five of the aerosol optical depth bins, which was considered insufficient for calculating trends, and was left blank in the figures. In Figures 1–3, the circles mark the results for the partly cloudy pixel retrievals and the crosses mark the results for the threshold retrievals.

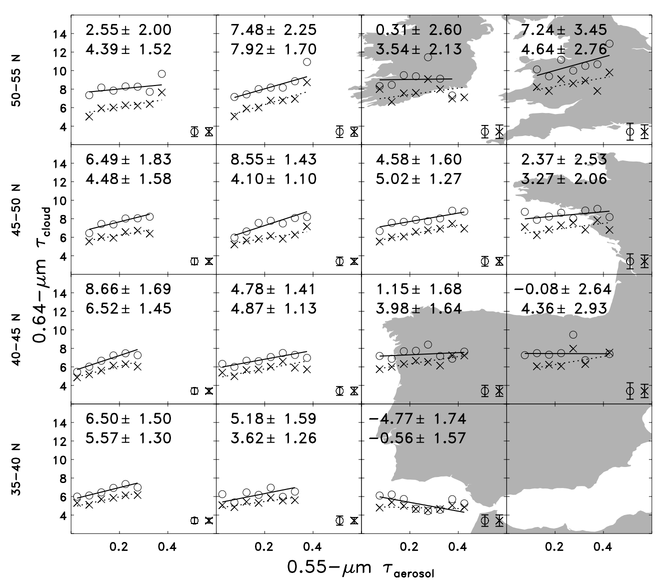

Figure 2. Same as Figure 1, but for 0.64-μm cloud optical depth.

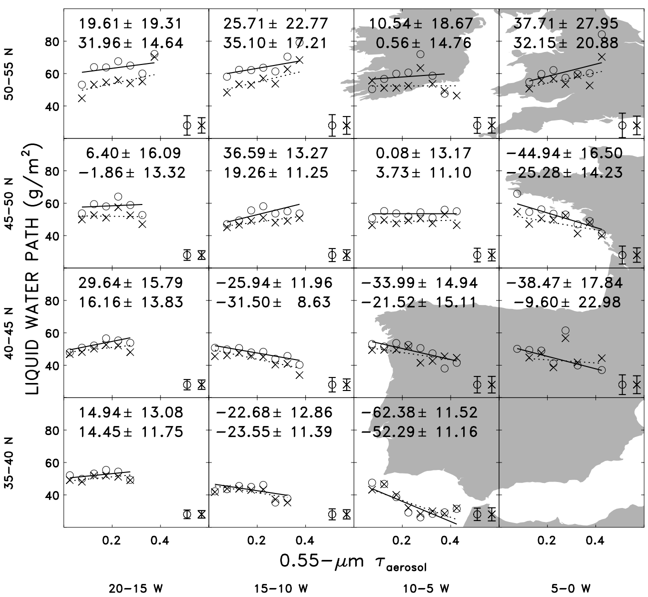

Figure 3. Same as Figure 1, but for liquid water path (g/m^2).

[10] Figure 1 shows that the cloud droplet effective radii obtained using threshold retrievals were generally larger, averaging 12.6 μm, than those retrieved with the partly cloudy pixel retrievals, averaging 11.2 μm. Droplet effective radius decreased as aerosol optical depth increased in most of the 5° regions. The mean slope, weighting the 15 regions equally, is −5.7 μm per unit change in aerosol optical depth for the partly cloudy pixel retrievals and −6.5 μm for the threshold retrievals. Assuming that each 5° region provides a statistically independent estimate, the difference in the mean slopes is significant at the 90% confidence level using a one-sided *t*-test.

[11] Figure 2 shows that the cloud optical depths obtained using threshold retrievals were smaller, averaging 6.0, than those obtained using the partly cloudy retrievals, averaging 7.2. In most of the 5° regions, cloud optical depth increased as aerosol optical depth increased. The mean slope is 4.1 per unit change in aerosol optical depth for the partly cloudy pixel retrievals and 4.4 for the threshold retrievals. The threshold retrievals amplify the change in cloud optical depth by about 10%, but owing to the large variability in the trends for the 15 regions, the difference in mean slopes is not statistically significant.

[12] Clearly, the biases reported here depend on the spatial resolution of the imager, the size of the region adopted for the collocation of aerosol and cloud properties, and the location and season chosen for the analysis. All of these factors influence the relative populations of cloud-free, partly cloudy, and overcast pixels, and consequently, estimates of the biases that arise from threshold cloud retrievals.

[13] Unlike the changes in droplet effective radius and cloud optical depth, the changes in liquid water path with increasing aerosol optical depth, as shown in Figure 3, were marginal in many of the 5° regions. Here, liquid water path was taken to be given by $W = \frac{2}{3}\tau_c R_e \rho$ with τ_c the cloud visible optical depth, R_e the droplet effective radius, and ρ the density of liquid water. Twomey's first estimate of the aerosol indirect radiative forcing assumed that cloud liquid water amounts were fixed [*Twomey*, 1974]. With the slopes of liquid water path smaller than their estimated uncertainties in many of the regions, fixed liquid water amounts would seem appropriate. *Albrecht* [1989], on the other hand, suggested that owing to the suppression of drizzle in clouds with smaller droplets, cloud liquid water would increase with increasing aerosol burden. While there was a tendency for an increase in liquid water paths for the maritime regions away from the continent, in only five of the 5° regions for the partly cloudy pixel retrievals and three for the threshold retrievals were the slopes of the trends with aerosol optical depth greater than twice the standard error of the slope. These regions were near the coast where the slopes were negative, indicating a decrease in cloud liquid water path with increasing aerosol optical depth. Air masses with larger aerosol burdens probably originated over the continent and were therefore likely to be dryer than the less polluted, oceanic air masses. *Ackerman et al.* [2004] suggested that when the air in the free troposphere above the clouds is sufficiently dry, polluted clouds could lose liquid water, as appears to occur near the coast for the results shown in Figure 3.

4. Radiative Forcing Estimates

[14] To investigate the impact of the trends in cloud optical depth and droplet effective radius with aerosol optical depth on estimates of the aerosol radiative forcing, top of the atmosphere fluxes were calculated in each of the 5° regions using a broadband radiative transfer model that accounts for scattering and absorption by gases, aerosols, and clouds [*Coakley et al.*, 2002]. The model was run twice without clouds, once with 0.55-μm aerosol optical depth set to 0.15, and once with the optical depth set to 0.25. The difference in the top of the atmosphere fluxes between these two cases was taken to represent the direct radiative forcing for cloud-free conditions due to the 0.1 increase in aerosol optical depth. The model was then run twice with overcast clouds overlying the aerosol, once with a cloud optical depth overlying an aerosol with an optical depth of 0.15 and again for clouds overlying an aerosol with an optical depth of 0.25. The difference in the top of the atmosphere fluxes between these cases was taken to represent the aerosol indirect radiative forcing for overcast conditions due to the 0.1 increase in aerosol optical depth. *Matheson et al.* [2005] reported that the contribution to the radiative forcing due to scattering and absorption by the additional aerosol in the column was small compared with the radiative forcing from changes in the clouds. The cloud optical depths were calculated using the given aerosol optical depths and the trend lines for both the threshold and partly cloudy pixel retrievals in Figure 2. The results are represented by squares in Figure 4. The overcast calculations were repeated using the same aerosol optical depths, but using the trend lines for changes in the droplet effective radius in Figure 1 which leads to changes in cloud optical depth for fixed cloud liquid water. The results are represented by pluses in Figure 4.

[15] The means of the forcing using the observed trends in cloud optical depth, weighting all 15 regions equally,

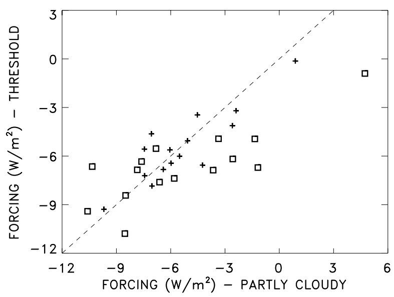

Figure 4. Radiative forcing estimates for overcast conditions (W/m^2) based on partly cloudy pixel and threshold retrievals for an increase in the 0.55-μm aerosol optical depth of 0.1 (from 0.15 to 0.25). Squares give the forcing based on changes in cloud optical depth taken from the linear fits in Figure 2. Pluses give the forcing based on changes in droplet effective radius taken from the linear fits in Figure 1 and an assumption of fixed liquid water amount.

were −5.3 W/m^2 for the partly cloud pixel retrievals and −6.6 W/m^2 for the threshold retrievals, an increase of 22%. The mean bias and RMS deviation were −1.3 and 2.9 W/m^2 respectively. The change in reflectivity of a cloud is approximately proportional to $\Delta\tau_c/\tau_c$ so that although $\Delta\tau_c$ was only 10% larger in the threshold retrievals, τ_c was 18% smaller, creating the 22% bias in radiative forcing when using the threshold retrievals. Clearly, the bias is small compared with the variability in the estimates of the forcing for the 15 regions. So, while estimates of the aerosol indirect radiative forcing are biased, this bias is small compared with effects due to other factors that govern the properties of the clouds and their apparent response to the aerosols, and as noted by *Matheson et al.* [2005], may govern the properties of the aerosols as well.

[16] Interestingly, the means of the forcing for overcast conditions when liquid water was held fixed were −5.4 W/m^2 for the partly cloudy pixel retrievals and −5.5 W/m^2 for the threshold retrievals. The mean bias was −0.1 W/m^2 and the RMS deviation was 1.2 W/m^2. The fractional change in cloud optical depth for fixed liquid water is equal to $-\Delta R_e/R_e$. Although ΔR_e was approximately 15 % larger for the threshold retrievals, R_e was also 12% larger. The biases in droplet effective radii and in the sensitivity of droplet radius to changes in aerosol optical depth in the threshold retrievals nearly cancel in the estimates of the aerosol indirect radiative forcing assuming fixed cloud liquid water path.

[17] **Acknowledgment.** This work was supported in part by the NASA *CALIPSO* Project through NAS1-99104, NASA grant NNG04GM11G, and the NOAA Global Change Program through NA16GP2911.

References

Ackerman, A. S., M. P. Kirkpatrick, D. E. Stevens, and O. B. Toon (2004), The impact of humidity above stratiform clouds on indirect aerosol climate forcing, *Nature*, *432*, 1014–1017.

Albrecht, B. A. (1989), Aerosols, cloud microphysics, and fractional cloudiness, *Science*, *245*, 1227–1230.

Bevington, P. R. (1969), *Data Reduction and Error Analysis for the Physical Sciences*, McGraw-Hill, New York.

Coakley, J. A. Jr., W. R. Tahnk, A. Jayaraman, P. K. Quinn, C. Devaux, and D. Tanré (2002), Aerosol optical depths and direct radiative forcing for INDOEX derived from AVHRR: Theory, *J. Geophys. Res.*, *107*(D19), 8009, doi:10.1029/2000JD000182.

Coakley, J. A. Jr., M. A. Friedman, and W. R. Tahnk (2005), Retrievals of cloud properties for partly cloudy imager pixels, *J. Atmos. Oceanic Technol.*, *22*, 3–17.

Kaufman, Y. J., and R. S. Fraser (1997), The effect of smoke particles on clouds and climate forcing, *Science*, *277*, 1636–1639.

Kaufman, Y. J., and T. Nakajima (1993), Effect of Amazon smoke on cloud microphysics and albedo—Analysis from satellite imagery, *J. Appl. Meteorol.*, *32*, 729–744.

Loeb, N. G., and N. Manalo-Smith (2005), Top-of-atmosphere direct radiative effect of aerosols over global oceans from merged CERES and MODIS observations, *J. Clim.*, *18*, 3506–3526.

Matheson, M. A., J. A. Coakley Jr., and W. R. Tahnk (2005), Aerosol and cloud property relationships for summertime stratiform clouds in the northeastern Atlantic from Advanced Very High Resolution Radiometer observations, *J. Geophys. Res.*, *110*, D24204, doi:10.1029/2005JD006165.

Nakajima, T., A. Higurashi, K. Kawamoto, and J. E. Penner (2001), A possible correlation between satellite-derived cloud and aerosol microphysical parameters, *Geophys. Res. Lett.*, *28*, 1171–1174.

Quaas, J., O. Boucher, and F.-M. Bréon (2004), Aerosol indirect effects in POLDER satellite data and the Météorologie Dynamique—Zoom (LMDZ) general circulation model, *J. Geophys. Res.*, *109*, D08205, doi:10.1029/2003JD004317.

Rossow, W. B., and L. C. Garder (1993), Cloud detection using satellite measurements of infrared and visible radiances for ISCCP, *J. Clim.*, *6*, 2341–2369.

Sekiguchi, M., T. Nakajima, K. Suzuki, K. Kawamoto, A. Higurashi, D. Rosenfeld, I. Sano, and S. Mukai (2003), A study of the direct and indirect effects of aerosols using global satellite data sets of aerosol and cloud parameters, *J. Geophys. Res.*, *108*(D22), 4699, doi:10.1029/2002JD003359.

Twomey, S. (1974), Pollution and the planetary albedo, *Atmos. Environ.*, *8*, 1251–1256.

Wetzel, M. A., and L. L. Stowe (1999), Satellite-observed patterns in stratus microphysics, aerosol optical thickness, and shortwave radiative forcing, *J. Geophys. Res.*, *104*(D24), 31,287–31,299.

J. A. Coakley Jr. and W. R. Tahnk, College of Oceanic and Atmospheric Sciences, 104 COAS Admin Building, Oregon State University, Corvallis, OR 97331-5503, USA. (coakley@coas.oregonstate.edu)

M. A. Matheson, Department of Environmental Engineering, Building Research Institute, 1 Tehara, Tsukuba, Ibaraki, 305-0802, Japan.